KYUNGPOOK Math. J. 60(2020), 335-347
https://doi.org/10.5666/KMJ.2020.60.2.335
pISSN 1225-6951 eISSN 0454-8124

Bifurcation Analysis of a Spatiotemporal Parasite-host System

Hunki Baek
Department of Mathematics Education, Daegu Catholic University, Gyeongsan, Gyeongbuk, 38430, Republic of Korea
e-mail : hkbaek@cu.ac.kr

Abstract. In this paper, we take into account a parasite-host system with reaction-diffusion. Firstly, we derive conditions for Hopf, Turing, and wave bifurcations of the system in the spatial domain by means of linear stability and bifurcation analysis. Secondly, we display numerical simulations in order to investigate Turing pattern formation. In fact, the numerical simulation discloses that typical Turing patterns, such as spotted, spot-stripelike mixtures and stripelike patterns, can be formed. In this study, we show that typical Turing patterns, which are well known in predator-prey systems ([7, 18, 25]), can be observed in a parasite-host system as well.

1. Introduction

It is widely known that parasites play an important role in reducing host density and in extinctionizing the host population in some cases([2, 8]). In order to describe such phenomena by means of mathematical models, Ebert et al. [8] suggested the following microparasite model

$$\begin{cases} \dfrac{dS}{dt} = a(S + bI)(1 - c(S + I)) - eS - \beta SI, \\ \dfrac{dI}{dt} = -(e + \alpha)I + \beta SI, \end{cases} \tag{1.1}$$

where S and I represent the densities of uninfected and infected hosts, respectively. The constant a is the maximum per capita birth rate of uninfected hosts, $b(0 \leq b \leq 1)$ is the relative fecundity of an infected host, c measures the per capita density-dependent reduction in birth rate, e is the parasite-independent host background

Received April 25, 2018; accepted March 7, 2020.
2010 Mathematics Subject Classification: 34C23, 37B55, 92D25, 92D30.
Key words and phrases: a spatiotemporal parasite-host system,Turing bifurcation, Hopf bifurcation, wave bifurcation, pattern formation.
This work was supported by research grants from the Catholic University of Daegu in 2017.

mortality, and α is the parasite-induced excess death rate and β is the constant infection rate.

From simple local stability analysis, we know that system (1.1) satisfying $a > d$ has always the saddle equilibrium $O(0,0)$, which implies that extinction of host is impossible under $a > d$. In addition, in [12], they have shown that system (1.1) predicts the existence of a globally attractive positive steady state. Thus it is not a suitable model to explain the extinction situation of the uninfected host.

After carefully investigating the infection term βSI, Hwang and Kuang [12] obtained the following system by replacing the mass action incidence function βSI with a standard incidence function $\beta \frac{SI}{S+I}$.

$$\begin{cases} \dfrac{dS}{dt} = a(S+bI)(1-c(S+I)) - eS - \beta \dfrac{SI}{S+I}, \\ \dfrac{dI}{dt} = -(e+\alpha)I + \beta \dfrac{SI}{S+I}, \end{cases} \tag{1.2}$$

where β represents the maximum number of infections that an infected host can cause per unit time. In [12, 21], the authors have studied about various dynamical behaviors of the revised system (1.2) including the fact that the host extinction and reduction dynamics can be exhibited.

Now, for simplicity, we nondimensionalizes the system (1.2) with the following scaling

$$\bar{t} = at, \bar{S} = cS, \bar{I} = cI, \tag{1.3}$$

and dropping the bar notation, then we have the following system:

$$\begin{cases} \dfrac{dS}{dt} = (S+bI)(1-S-I) - \delta S - h\dfrac{SI}{S+I} \equiv P(S,I), \\ \dfrac{dI}{dt} = -(\delta+r)I + h\dfrac{SI}{S+I} \equiv Q(S,I), \end{cases} \tag{1.4}$$

where $h = \frac{\beta}{a}, \delta = \frac{d}{a}, r = \frac{\alpha}{a}$.

Since $\lim_{(S,I)\to(0,0)} P(S,I) = \lim_{(S,I)\to(0,0)} Q(S,I) = 0$ we define that $P(0,0) = Q(0,0) = 0$. With this assumption, we know that both P and Q are continuous on the closure of $\mathbb{R}^2_+$ and C^1 smooth in $\mathbb{R}^2_+$ where $\mathbb{R}^2_+ = \{(x,y)|x > 0, y > 0\}$. Thus, standard arguments yields that the solutions of system (1.4) are positive, bounded and defined on $[0,\infty)$.

Although system (1.4) has been investigated by researchers [12, 16, 21] about its dynamics as an ordinary differential systems, one cannot infer any information about spatial distributions from such systems. Thus, it is needed to investigate spatial system. In fact, recently, many researchers have investigated spatiotemporal pattern formations and bifurcation analysis of spatiotemporal predator-prey systems [1, 3, 4, 5, 10, 15, 18, 20, 19, 25, 23, 22, 24, 26]. Thus, in this paper, we will take into account the following a parasite-host system with reaction-diffusion:

$$\begin{cases} \dfrac{dS}{dt} = D_1\nabla^2 S + (S+bI)(1-S-I) - \delta S - h\dfrac{SI}{S+I} \ \text{ in } \ \Omega, \\ \dfrac{dI}{dt} = D_2\nabla^2 I - (\delta+r)I + h\dfrac{SI}{S+I} \ \text{ in } \ \Omega, \end{cases} \tag{1.5}$$

where D_1 and D_2 are diffusion coefficients, $\nabla^2 = \frac{\partial^2}{\partial S^2} + \frac{\partial^2}{\partial I^2}$ is the usual Laplacian in two-dimensional space Ω and S, I stand for the space . Throughout the paper, we assume that system (1.5) has the Neumann boundary conditions as follows:

$$\frac{\partial S}{\partial n} = \frac{\partial I}{\partial n} = 0 \ \text{ on } \partial\Omega, \tag{1.6}$$

which means that no external input is imposed from outside.

The purposes of this paper are to investigate three bifurcation phenomena, Hopf, Turing and wave bifurcations, of system (1.5) and to give numerical simulations in order to observe Turing patterns caused by Turing bifurcation. In fact, in section , we establish the conditions for Hopf, Turing and wave bifurcations by using linear stability theory and bifurcation analysis and, in section 3, we analyze numerically typical Turing patterns via numerical simulations.

2. Linear Stability Analysis and Hopf Bifurcation of System (1.4)

In order to investigate bifurcation phenomena of system (1.5), first we have to consider the nonspatial system (1.4) of system (1.5). In fact, by setting $P(S,I) = 0, Q(S,I) = 0$ in system (1.4), we figure out that the nonspatial system (1.4) has at most three nonnegative equilibria as follows;

(i) $E_0 = (0, 0)$,

(ii) $E_1 = (1-\delta, 0)$ if $0 < \delta < 1$,

(iii) $E^* = (S^*, I^*)$ if $h > \delta + r$ and $bh + (\delta+r)(r+1) > (b+h)(\delta+r)$,

where

$$\begin{aligned} S^* &= \frac{\delta+r}{h-\delta-r} I^*, \\ I^* &= \frac{(h-\delta-r)(b(h-\delta-r) - (\delta+r)(h-r-1))}{h(bh+(1-b)(\delta+r))}. \end{aligned} \tag{2.1}$$

Here E_1 represents that there are no infected hosts and E^* implies that host is infected chronically. Since the local stability of equilibria E_0, E_1 and E^* is determined by the eigenvalues of the variational matrix, we need to consider the variational matrix of system (1.5) at a point $(x, y) \in \Omega$ given by

(2.2)
$$J(x,y) = \begin{pmatrix} \frac{\partial P}{\partial S} & \frac{\partial P}{\partial I} \\ \frac{\partial Q}{\partial S} & \frac{\partial Q}{\partial I} \end{pmatrix}_{(x,y)}$$
$$= \begin{pmatrix} 1-\delta-2x-(1+b)y-\frac{hy^2}{(x+y)^2} & b-(1+b)x-2by-\frac{hx^2}{(x+y)^2} \\ \frac{hy^2}{(x+y)^2} & -(\delta+r)+\frac{hx^2}{(x+y)^2} \end{pmatrix}.$$

From [12], the stability of the equilibrium E_0 can be obtained as shown in the following proposition.

Proposition 2.1. *For system* (1.4)*, the following statements are true.*

(a) *If $h \le \delta + r$ and $\delta \ge 1$, then E_0 is globally asymptotically stable.*

(b) *If $h > r+1$ and $bh+(\delta+r)(r+1) < (b+h)(\delta+r)$, then E_0 is globally stable.*

Now we consider the stability of the equilibrium E_1 in the following proposition.

Proposition 2.2. *Let $0 < \delta < 1$ in system* (1.4)*. Then the following statements are true.*

(a) *If $h < \delta + r$, then E_1 is globally asymptotically stable.*

(b) *If $h > \delta + r$, then E_1 is a saddle point.*

(c) *If $h = \delta + r$, then E_1 is a saddle node.*

Proof. Parts (a) and (b) follow from [12] and the variational matrix defined by

$$J(E_1) = \begin{pmatrix} \delta-1 & b \\ 0 & h-(\delta+r) \end{pmatrix}. \tag{2.3}$$

Now, let $h = \delta + r$ for the part (c). Then the trace of the matrix $J(E_1)$ is not zero, one of the eigenvalues of the matrix $J(E_1)$ is zero and the other is nonzero. Thus in order to determine the dynamics of system (1.4) in the neighborhood of the equilibrium E_1, we transform the equilibrium E_1 to the origin and then expand the right hand side of system (1.4) as a Taylor series. Then system (1.4) can be written as

$$\begin{cases} \frac{dS}{dt} =(\delta-1)S+(b\delta-r-1)I-S^2+\frac{b(1-\delta)-\delta-r}{\delta-1}I^2 \\ \qquad -(b+1)SI+P_1(S,I), \\ \frac{dI}{dt} =\frac{\delta+r}{\delta-1}I^2+Q_1(S,I), \end{cases} \tag{2.4}$$

where $P_1(S, I)$ and $Q_1(S, I)$ are C^∞ functions of order at least three in (S, I). Let $S = x - (b\delta - r - 1)y$, $I = (\delta - 1)y$ and $\tau = (\delta - 1)t$, then system (2.4) can be transformed into the following system:

$$(2.5)\quad \begin{cases} \dfrac{dx}{d\tau} = x - \dfrac{1}{\delta-1}x^2 + \dfrac{(b(\delta+1)-\delta-2r-1)}{\delta-1}xy \\ \quad + \dfrac{((-1+b)\delta^2+(b-2r-1)r-\delta(b^2+3r+1-2b(r+1)))}{\delta-1}y^2 \\ \quad + P_2(x,y), \\ \dfrac{dy}{d\tau} = \dfrac{(\delta+r)}{\delta-1}y^2 + Q_2(x,y), \end{cases}$$

where $P_2(x,y)$ and $Q_2(x,y)$ are C^∞ functions of order at least three in (x,y). Now using Theorem 7.1 of Chapter 2 in [27] , we can obtain that E_1 is a saddle node. □

In the following proposition, we mention the local stability of the equilibrium E^* obtained from [12].

Proposition 2.3. *For system* (1.4)*, the following statements are true.*

(a) *If $\delta + r < h \leq r+1$, then E^* is globally asymptotically stable.*

(b) *If $h > r+1$ and $bh + (\delta+r)(r+1) > (b+h)(\delta+r)$, then E^* is globally stable.*

Now we can investigate Hopf-bifurcation phenomenon around the equilibrium E^* in the following theorem.

Theorem 2.4. *System* (1.4) *can have a Hopf-bifurcation around E^* at $b = b_H$ if*

$$(2.6)\qquad \Gamma_1 - \Gamma_2 - \Gamma_3 \neq 0$$

where b_H satisfies the following equality of b

$$1 - 2\delta + h - r - \frac{2h}{\theta+1} - \gamma = 0$$

and

$$\begin{aligned} \theta &= \frac{\delta+r}{h-\delta-r}, \\ \gamma &= \frac{(-\delta+h-r)(-(-1+h-r)(\delta+r)-b(\delta-h+r))(1+b+2\theta)}{h(bh-(-1+b)(\delta+r))}, \\ \Gamma_1 &= \frac{(h-r)(\delta+r)(\delta-h+r)(\delta-b_H\delta+h+b_Hh+r-b_Hr)}{h(\delta-b_H\delta+b_Hh+r-b_Hr)^2}, \\ \Gamma_2 &= \frac{2(h-r)(\delta+r)(\delta-h+r)(\delta+r+(\delta-h+r)\theta)}{\Gamma_3((-1+b_H)\delta-b_Hh+(-1+b_H)r)^2(1+\theta)^2}, \\ \Gamma_3 &= \frac{(h-\delta-r)(b_H(h-\delta-r)-(\delta+r)(h-r-1))}{h(b_Hh+(1-b_H)(\delta+r))}. \end{aligned}$$

Proof. Consider the characteristic equation at the equilibrium point E^* as follows:

$$\lambda^2 - \text{tr}(J(E^*))\lambda + \det(J(E^*)) = 0 \tag{2.7}$$

where $\text{tr}(J(E^*))$ and $\det(J(E^*))$ is the trace and the determinant of the of the variational matrix $J(E^*)$ of the point E^*, respectively. If $\text{tr}(J(E^*)) = 0$ at $b = b_H$, then both the eigenvalues, the solutions of the equation (2.7), become purely imaginary under the condition $\det(J(E^*)) > 0$. Now, replacing $\lambda = \lambda_1 + i\lambda_2$ into the equation (2.7) and then from separating real and imaginary parts we can get the followings:

$$(\lambda_1^2 - \lambda_2^2) - \text{tr}(J(E^*))\lambda_1 + \det(J(E^*)) = 0, \tag{2.8a}$$

$$2\lambda_1\lambda_2 - \text{tr}(J(E^*))\lambda_2 = 0. \tag{2.8b}$$

From elementary differentiation of (2.8b) with respect to b and considering $\lambda_1 = 0$, we get

$$\frac{d\lambda_1}{db}\Big|_{b=b_H} = \Gamma_1 - \Gamma_2 - \Gamma_3$$

where

$$\begin{aligned}
\theta &= \frac{\delta + r}{h - \delta - r},\\
\Gamma_1 &= \frac{(h-r)(\delta+r)(\delta-h+r)(\delta - b_H\delta + h + b_H h + r - b_H r)}{h(\delta - b_H\delta + b_H h + r - b_H r)^2},\\
\Gamma_2 &= \frac{2(h-r)(\delta+r)(\delta-h+r)(\delta + r + (\delta - h + r)\theta)}{\Gamma_3((-1+b_H)\delta - b_H h + (-1+b_H)r)^2(1+\theta)^2},\\
\Gamma_3 &= \frac{(h-\delta-r)(b_H(h-\delta-r) - (\delta+r)(h-r-1))}{h(b_H h + (1-b_H)(\delta+r))}.
\end{aligned}$$

Thus it follows from (2.6) that $\frac{d\lambda_1}{db}\Big|_{b=b_H} \neq 0$. Therefore, by Poincar$\acute{e}$-Andronov-Hopf Theorem [11], system (1.4) goes through a Hopf-bifurcation at $b = b_H$ around E^*. □

3. Turing and Wave Bifurcations of System (1.5)

In this section we consider the spatiotemporal parasite-host system (1.5) in order to look into Turing and wave bifurcations. For this, we will perform a linear stability analysis for system (1.5) around the nontrivial stationary state (S^*, I^*) by linearizing the dynamical system (1.5) around the spatially homogeneous fixed point (S^*, I^*) for small space- and time-dependent fluctuations and expand them in Fourier space. Now, let

$$\begin{aligned}
S(\vec{x}, t) &\sim S^* e^{\lambda t} e^{i\vec{k}\cdot\vec{x}},\\
I(\vec{x}, t) &\sim I^* e^{\lambda t} e^{i\vec{k}\cdot\vec{x}},
\end{aligned} \tag{3.1}$$

where $\vec{x} = (S, I)$, λ is the growth rate of perturbation in time t and $\vec{k} = (k_S, k_I)$ is the wave number vector. Let $\vec{k} \cdot \vec{k} = k_S^2 + k_I^2 \equiv k^2$. Then we can obtain the corresponding characteristic equation as follows:

$$|J_k - \lambda E| = 0, \tag{3.2}$$

where $J_k = J(E^*) - k^2 D$, E is the identity matrix and $D = \text{diag}(D_1, D_2)$ is the diffusion matrix and $J(E^*)$ is given in (2.2) as

$$J(E^*) = \begin{pmatrix} \frac{\partial P}{\partial S} & \frac{\partial P}{\partial I} \\ \frac{\partial Q}{\partial S} & \frac{\partial Q}{\partial I} \end{pmatrix}_{(S^*, I^*)} \equiv \begin{pmatrix} P_S & P_I \\ Q_S & Q_I \end{pmatrix}. \tag{3.3}$$

Equation (3.2) can be solved, yielding the characteristic polynomial

$$\lambda^2 - \text{tr}(J_k)\lambda + \det(J_k) = 0, \tag{3.4}$$

where

$$\begin{aligned} \text{tr}(J_k) &= P_S + Q_I - k^2(D_1 + D_2) \quad \text{and} \\ \det(J_k) &= P_S Q_I - P_I Q_S - k^2(D_1 Q_I + D_2 P_S) + k^4 D_1 D_2. \end{aligned} \tag{3.5}$$

The solutions of equation (3.4) yield the dispersion relation

$$\lambda_k^{\pm} = \frac{1}{2}\Big(\text{tr}(J_k) \pm \sqrt{\text{tr}(J_k)^2 - 4\det(J_k)}\Big). \tag{3.6}$$

The reaction-diffusion systems have led to the characterization of three basic types of symmetry-breaking bifurcations-Hopf , Turing and wave bifurcation, which are responsible for the emergence of spatiotemporal patterns [1, 5, 6, 10, 14, 15, 18, 20, 19, 25, 23, 22, 24]).

3.1. Turing Bifurcation

Turing bifurcation(or called Turing instability) is a phenomenon that causes certain reaction-diffusion system to lead to spontaneous stationary configuration. It is why Turing instability is often called *diffusion-driven instability.* Turing instability is not dependent on the geometry of the system but only on the reaction rates and diffusion. It can occur only when the inhibitor(S) diffuses faster than the activator(I) [15, 25, 23].

In fact, Turing instability sets in when at leat one of the solutions of equation (3.4) crosses the imaginary axis. In other words, the spatially homogeneous steady state will become unstable due to heterogeneous perturbation when at least one solution of equation (3.4) is positive. For the reason, at least one out of the following two inequalities is violated to occur the Turing instability phenomenon:

$$\begin{aligned} \text{tr}(J_k) &= P_S + Q_I - (D_1 + D_2)k^2 < 0, \\ \det(J_k) &= D_1 D_2 k^4 - (D_1 Q_I + D_2 P_S)k^2 + P_S Q_I - P_I Q_S > 0. \end{aligned} \tag{3.7}$$

Thus we can get the conditions for Turing bifurcation in the following theorem.

Theorem 3.1. *Suppose that* $h > \delta + r$ *and* $bh + (\delta + r)(r + 1) > (b + h)(\delta + r)$ *hold. Then Turing bifurcation occurs if*

$$-\frac{1}{4D_1D_2}\big(D_1(\delta - h + 2\eta - \frac{\eta^2}{h} + r) + D_2(\delta - 1 + \frac{\eta^2}{h} + \frac{\theta_2}{\theta_1}(2 + \frac{\eta}{h}(b-1)))\big)^2 + \frac{\theta_2}{\theta_1}\big(2(\delta - h) + (5-b)\eta + 2r + \frac{(b-1)\eta}{h}(\delta + 3\eta + r)\big) + (\delta - 1)(\delta + 2\eta + r - h) + \frac{\eta^2}{h}(1 - b + r) < 0$$

is satisfied. Here $\eta = h - \delta - r, \theta_1 = b\eta + \delta + r, \theta_2 = \theta_1 - (h - \eta)(h - r)$.

Proof. From the hypotheses and Proposition , we know that there exists the positive non-spatial steady state E^* which is stable. Thus $\operatorname{tr}(J(E^*)) = P_S + Q_I < 0$ and $\det(J(E^*)) = P_SQ_I - P_IQ_S > 0$ are satisfied. It is seen from these facts that the first condition in (3.7) always holds. Hence we are left only one for the instability condition, i.e.,$T(k^2) \equiv \det(J_k) < 0$. Elementary calculations yield that

$$\begin{aligned} T(k^2) = \big(&D_1(\delta - h + 2\eta - \frac{\eta^2}{h} + r) + D_2(\delta - 1 + \frac{\eta^2}{h} + \frac{\theta_2}{\theta_1}(2 + \frac{\eta}{h}(b-1)))\big)k^2 \\ &+ \frac{\theta_2}{\theta_1}\big(2(\delta - h) + (5-b)\eta + 2r + \frac{(b-1)\eta}{h}(\delta + 3\eta + r)\big) \\ &+ (\delta - 1)(\delta + 2\eta + r - h) + \frac{\eta^2}{h}(1 - b + r) + D_1D_2k^4 \end{aligned} \tag{3.8}$$

where

$$\eta = h - \delta - r, \theta_1 = b\eta + \delta + r, \theta_2 = \theta_1 - (h - \eta)(h - r).$$

Thus the minimum of $T(k^2)$ occurs at the critical wavenumber k_T^2, where

(3.9)

$$\begin{aligned} k_T^2 &= -\frac{1}{2D_1D_2}\big(D_1(\delta - h + 2\eta - \frac{\eta^2}{h} + r) + D_2(\delta - 1 + \frac{\eta^2}{h} + \frac{\theta_2}{\theta_1}(2 + \frac{\eta}{h}(b-1)))\big), \\ \eta &= h - \delta - r, \theta_1 = b\eta + \delta + r, \theta_2 = \theta_1 - (h - \eta)(h - r). \end{aligned}$$

By substituting $k^2 = k_T^2$ into $T(k^2)$, we can get a sufficient condition for the Turing instability as follows:

(3.10)

$$\begin{aligned} T(k^2) = \big(&D_1(\delta - h + 2\eta - \frac{\eta^2}{h} + r) + D_2(\delta - 1 + \frac{\eta^2}{h} + \frac{\theta_2}{\theta_1}(2 + \frac{\eta}{h}(b-1)))\big)k^2 \\ &+ \frac{\theta_2}{\theta_1}\big(2(\delta - h) + (5-b)\eta + 2r + \frac{(b-1)\eta}{h}(\delta + 3\eta + r)\big) \\ &+ (\delta - 1)(\delta + 2\eta + r - h) + \frac{\eta^2}{h}(1 - b + r) + D_1D_2k^4 < 0. \end{aligned}$$

□

Remark 3.2. We can find out the critical value of bifurcation parameter δ for Turing bifurcation by replacing the inequality in (3.10) with the equality. Thus the critical value δ_T has to be satisfied with the following equation;

(3.11)
$$\frac{1}{4D_1D_2}\big(D_1(\delta_T - h + 2\eta - \frac{\eta^2}{h} + r) + D_2(\delta_T - 1 + \frac{\eta^2}{h} + \frac{\theta_2}{\theta_1}(2 + \frac{\eta}{h}(b-1)))\big)^2$$
$$= (\delta_T - 1)(\delta_T + 2\eta + r - h) + \frac{\eta^2}{h}(1 - b + r)$$
$$+ \frac{\theta_2}{\theta_1}\big(2(\delta_T - h) + (5-b)\eta + 2r + \frac{(b-1)\eta}{h}(\delta_T + 3\eta + r)\big).$$

At the Turing threshold δ_T, the spatial symmetry of the system is broken and the patterns are stationary in time and oscillatory in space with the wavelength

$$\lambda_T = \frac{2\pi}{k_T}. \tag{3.12}$$

3.2. Wave Bifurcation

The wave instability caused by the wave bifurcation plays an important part in pattern formations in many areas [20, 19, 26]. Similar to the Hopf bifurcation the wave bifurcation take places when a pair of imaginary eigenvalues across the real axis from the negative the positive side for $k = k_w \neq 0$ in equation (3.4). Thus we can get the conditions for the wave bifurcation in the following theorem.

Theorem 3.3. *Wave bifurcation occurs if $\delta > \delta_w$, where*

$$\delta_w = \frac{L + h\sqrt{M}}{2(b-1)(b+h-r-1)}.$$

Here,

$$L = h(D_1 + D_2)(b-1)k^2$$
$$+ 2(b^2(h-r) + (h-r-1)r + b(h^2 + r(r+2) - h(2r+1))),$$
$$M = ((D_1 + D_2)(b-1))^2k^4 + 4b(h-r)(b+h-r-1).$$

Proof. In order that system (1.5) has a wave bifurcation, equation (3.4) must have purely imaginary roots when $k \neq 0$. In other words, the wave bifurcation occurs if the following conditions are satisfied:

$$\mathrm{Im}(\lambda_k) \neq 0 \text{ and } \mathrm{Re}(\lambda_k) = 0 \text{ at } k = k_w \neq 0. \tag{3.13}$$

Thus, from elementary calculation, the critical value of wave bifurcation parameter δ can be obtained as

$$\delta_w = \frac{L + h\sqrt{M}}{2(b-1)(b+h-r-1)} \tag{3.14}$$

where

$$(3.15)\qquad \begin{aligned} L &= h(D_1+D_2)(b-1)k_w^2 \\ &\quad + 2(b^2(h-r)+(h-r-1)r+b(h^2+r(r+2)-h(2r+1))), \\ M &= ((D_1+D_2)(b-1))^2k_w^4+4b(h-r)(b+h-r-1). \end{aligned} \qquad \square$$

Remark 3.4. In fact, at the wave threshold δ_2, both spatial and temporal symmetries are broken and the patterns are oscillatory in space and time with the wave length λ_w satisfying

$$\lambda_w = \frac{2\pi}{k_w}, k_w^2 = \frac{1}{D_1+D_2}(P_S+Q_I)(\mathrm{tr}(J_k)=0).$$

4. Numerical Simulation : Turing pattern

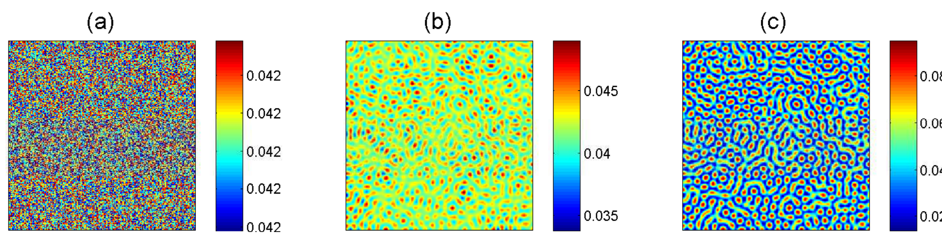

Figure 1: Snapshots of contour pictures of the time evolution of the uninfected population in system (1.5) when $\delta = 0.5$: (a) 0 iteration; (b) 30000 iterations; (c) 49000 iterations

In this section, we display numerical simulations of the spatiotemporal parasite-host system (1.5) to investigate spatiotemporal pattern formations caused by Turing bifurcation.

For this, we adopt a finite difference numerical method for the spatial derivatives, an explicit Euler method for the time integration and no-flux boundary condition for the boundary condition. Also we use a finite nondimensional domain of $[0, 200] \times [0, 200]$, and the space step $\Delta x = \Delta y = 0.25$ and the time step $\Delta t = 0.01$ which satisfy the CFL(Courant - Friedrichs-Lewy) stability criterion for two dimensional diffusion equations [9, 13]. It is well known that spatiotemporal dynamics of a diffusion-reaction system depends on the choice of initial conditions [17]. It seems to be reasonable from the biological point of view that the initial density distribution is taken as a small amplitude random perturbation around the steady state $E^* = (S^*, I^*)$. We run the numerical simulations until the numerical solutions

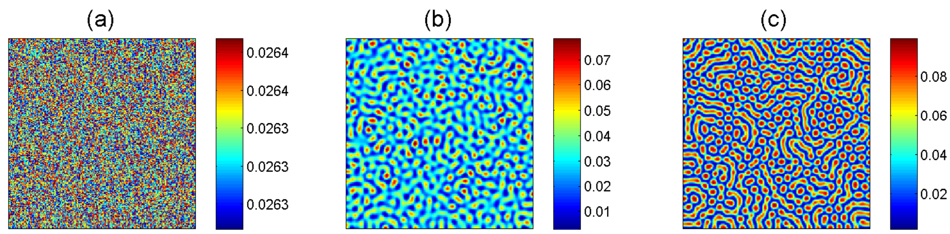

Figure 2: Snapshots of contour pictures of the time evolution of the uninfected population in system (1.5) when $\delta = 0.7$: (a) 0 iteration; (b) 15000 iterations; (c) 49000 iterations

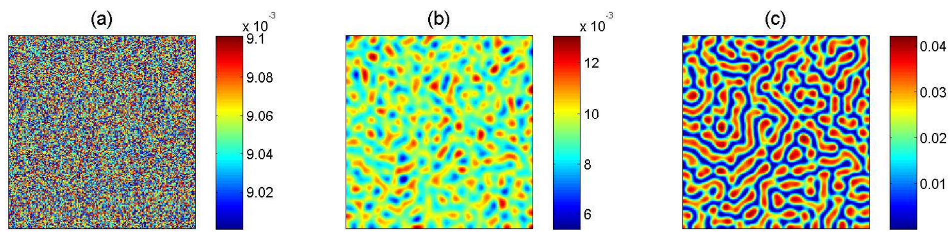

Figure 3: Snapshots of contour pictures of the time evolution of the uninfected population in system (1.5) when $\delta = 0.9$: (a) 0 iteration; (b) 15000 iterations; (c) 49000 iterations

either reach a stationary state or show a behavior that does not seem to change its characteristic anymore. In the numerical simulation, we have figured out that the distributions of uninfected and infected population are always of the same type. Thus we pay attention to the pattern formation of the uninfected population.

In order to illustrate Turing patterns numerically, first, we fix parameter values in system (1.5) as follows;

$$b = 0.1, h = 1.1, r = 0.1, D_1 = 0.1, D_2 = 1.0. \tag{4.1}$$

If we take the parameter value $\delta = 0.5$, we can observe that the random initial distribution is transformed into a regular spotted pattern, as shown in Figure 1. On the other hand, in Figure 2, we can see the existence of the steady state having the spotted pattern and the stripelike pattern simultaneously when the value $\delta = 0.7$ is chosen. Also Figure 3 shows that stripelike spatial patterns are prevalent in the whole domain eventually for the value $\delta = 0.9$.

Thus from these figures we can infer that Turing bifurcation causes three typical Turing patterns such as spotted, spot-stripe mixture, and stripelike patterns of the uninfected population in system (1.5) accordingly to the value δ. In this study, we show that typical Turing patterns, which are well known in a predator-prey system [7, 18, 25], can be investigated in a parasite-host system as well.

References

[1] D. Alonso, F. Bartumeus and J. Catalan, *Mutual interference between predators can give rise to Turing spatial patterns*, Ecology, **83(1)**(2002), 28–34.

[2] R. M. Anderson and R. M. May, *The population dynamics of microparasites and their invertebrate hosts*, Phil. Tran. R. Soc. Lond. B, **291**(1981), 451–524.

[3] H. Baek, *On the dynamical behavior of a two-prey one-predator system with two-type functional responses*, Kyungpook Math. J., **53(4)**(2013), 647-–660.

[4] H. Baek, *Spatiotemporal Dynamics of a Predator-Prey System with Linear Harvesting Rate*, Math. Probl. Eng., (2014), Art. ID 625973, 9 pp.

[5] M. Baurmann, T. Gross and U. Feudel, *Instabilities in spatially extended predator-prey systems : Spatio-temporal patterns in the neighborhood of Turing−Hopf bifurcations*, J. Theoret. Biol., **245**(2007), 220–229.

[6] I. Berenstein, M. Dolnik, L. Yang, A. M. Zhabotinsky, and I. R. Epstein, *Turing pattern formation in a two-layer system: Superposition and superlattice patterns*, Physical Review E, **70**(2004), 046219.

[7] B. I. Camara and M. A. Aziz-Alaoui, *Turing and Hope patterns formation in a predator-prey model with Leslie-Gower-type functional response*, Dynamics of Continuous, Discrete and Impulsive Systems Series B: Algorithms and Applications, **16**(2009), 479–488.

[8] D. Ebert, M. Lipsitch and K. L. Mangin, *The effect of parasites on host population density and extinction: experimental epidemiology with Daphnia and six microparasites*, Am. Nat., **156**(2000), 459–477.

[9] M. R. Garvie, *Finite-Difference schemes for reaction-diffusion equations modeling predator-prey interactions in MATLAB*, Bull. Math. Biol., **69**(2007), 931–956.

[10] D. A. Garzon-Alvarado, C. H. Galeano and J. M. Mantilla, *Turing pattern formation for reaction-convection-diffusion systems in fixed domains submitted to toroidal velocity fields*, Appl. Math. Model., **35**(2011), 4913–4925.

[11] J. Hale and H. Kocak, *Dynamics and bifurcations*, Springer-Verlag, New York, 1991.

[12] T.-W. Hwang and Y. Kuang, *Deterministic extinction effect of parasites on host populations*, J. Math. Biol., **46**(2003), 17–30.

[13] I. Kozlova, M. Singh, A. Easton and P. Ridland, *Twospotted spider mite predator-prey model*, Math. Comput. Model., **42**(2005), 1287–1298.

[14] L. Li, *Patch invasion in a spatial epidemic model*, Appl. Math. Comput., **258**(2015), 342–349.

[15] L. Li and Z. Jin, *Pattern dynamics of a spatial predator-prey model with noise*, Nonliear Dynam., **67(3)**(2012), 1737–1744.

[16] J. Li, Y. Xiao and Y. Yang, *Global analysis of a simple parasite-host model with homoclinic orbits*, Math. Biosci. Eng., **9(4)**(2012), 767–784.

[17] A. B. Medvinsky, S. V. Petrovskii, I. A. Tikhonova, H. Malchow and B.-L. Li, *Spatiotemporal complexity of plankton and fish dynamics*, SIAM Rev., **44(3)**(2002), 311–370.

[18] F. Rao, W. Wang and Z. Li, *Spatiotemporal complexity of a predator-prey system with the effect of noise and external forcing*, Chaos, Solitons Fractals, **41**(2009), 1634–1644.

[19] M. J. Smith, J. D. M. Rademacher and J. A. Sherratt, *Absolutes stability of wavetrains can explain spatiotemporal dynamics in reaction-diffusion systems of lambda-omega type*, SIAM J. Appl. Dyn. Syst., **8(3)**(2009), 1136–1159.

[20] M. J. Smith, J. A. Sherratt, *The effects of unequal diffusion coefficients on periodic travelling waves in oscillatory reaction-diffusion systems*, Physica D, **236**(2007), 90–103.

[21] K. Wang and Y. Kuang, *Fluctuation and extinction dynamics in host-microparasite systems*, Commun. Pure Appl. Anal., **10(5)**(2011), 1537–1548.

[22] W. Wang, W. Li, Z. Li and H. Zhang, *The effect of colored noise on spatiotemporal dynamics of biological invasion in a diffusive predator-prey system*, Biosystems, **104**(2011), 48–56.

[23] W. Wang, Q.-X. Liu and Z. Jin, *Spatiotemporal complexity of a ratio-dependent predator-prey system*, Phys. Rev. E, **75**(2007), 051913, 9 pp.

[24] Y. Wang, J. Wang and L. Zhang, *Cross diffusion-induced pattern in an SI model*, Appl. Math. Comput., **217**(2010), 1965–1970.

[25] W. Wang, L. Zhang, H. Wang and Z. Li, *Pattern formation of a predator-prey system with Ivlev-type functional response*, Ecological Modelling, **221**(2010), 131–140.

[26] L. Yang, M. Dolnik, A. M. Zhabotinsky and I. R. Epstein, *Pattern formation arising from interactions between Turing and wave instabilities*, J. Chem. Phys., **117(15)**(2002), 7259–7265.

[27] Z. F. Zhang, T. R. Ding, W. Z. Huang, Zh. X. Dong, *Qualitative theory of differential equations*, Translations of Mathematical Monographs **101**, AMS, Providence, RI, 1992.